J Mater Sci: Mater Electron **(2025) 36:634**

Experimental and theoretical investigation of gamma radiation absorption properties of oxide nanoparticles

Arzu Poyraz[1], Ibrahim Yigitoglu[2], Betul Canimkurbey[3,6], and Betul Cetin[4,5,*]

[1] *Vocational School of Health Services Department, Toros University, 33100 Mersin, Turkey*
[2] *Faculty of Arts and Sciences, Gaziosmanpaşa University, 60000 Tokat, Turkey*
[3] *Sabuncuoğlu Şerefeddin Health Services Vocational School, Amasya University, 05100 Amasya, Turkey*
[4] *Faculty of Arts and Sciences, Amasya University, 05100 Amasya, Turkey*
[5] *Faculty of Engineering, Amasya University, 05100 Amasya, Turkey*
[6] *Polatli Faculty of Arts and Sciences, Ankara Haci Bayram Veli University, 06570 Ankara, Turkey*

Received: 17 December 2024
Accepted: 17 March 2025
Published online: 10 April 2025

© The Author(s), 2025

ABSTRACT

With the development of technology, people are exposed to radiation in many areas throughout their lives. In order to minimize the damages of gamma rays, materials are being developed for shielding as well as dose limitation. For this reason, the glass sample was coated with a solution prepared with CuO, ZnO, and TiO_2 at a ratio of 1:1:3 to a 50% ZrB_2.50%PbO mixture, respectively. The radiation parameters of the prepared samples were examined experimentally with NaI (Tl) detector gamma spectrometry. Na-22 (511 keV, 1274 keV), Cs-137 (662 keV), and Co-60 (1173 keV, 1332 keV) radioactive point sources were used in the shielding experiments. The experimentally obtained radiation shielding parameters (linear attenuation coefficient, half value layer and mean free path) were compared with the theoretically calculated values in the Geant4-based GATE simulation program and the XCOM program. Experimental and theoretical values were found to be compatible with each other.

1 Introduction

The advancement of technology day by day has led to an increase in devices that work with radiation in almost every field. Minimizing the amount of additional radiation, which is a result of advancing technology, is possible with shielding; this is the most important of the three basic principles of radiation protection. Shielding is to reduce the intensity of radiation to minimum levels by placing a radiation absorbing material between the radioactive source and the living being in order to protect from the radioactive source or to minimize exposure. For this purpose, many materials such as concrete, marble, granite and alloys are used in gamma ray shielding processes. Experimental and theoretical studies on the radiation protection properties of materials such as zeolite [1], granite [2], polyurethane [3], colemanite, barite, ground basaltic

Address correspondence to E-mail: betulcetin3205@gmail.com

https://doi.org/10.1007/s10854-025-14691-5

pumice and ground blast furnace slag [4], soda-lime-silica glasses doped with different food materials [5] are found in the literature. While the cheapness and easy availability of these materials is a great advantage, they also have disadvantages such as their inability to transmit visible light, strength, crack formation and water permeability [6],[7].

On the other hand, in recent years, there has been a significant increase in the use of glass and glass-based materials for radiation protection. Glass materials are one of the appropriate materials that may be used for radiation shielding because of its high transparency to visible light, hardness, it has relatively high densities, superior corrosion resistance, it can be formed in great volumes and controllable properties with changing compositions [6] With the increasing diversity in the application areas of glass structures with different compositions, glass and glass-based materials have become the focus of radiation shielding studies. Several studies have been undertaken in the literature. For example, silicate and borate heavy metal oxide glasses [8], gadolinium-based glasses [9], zinc borotellurite glasses [10], SnO-reinforced silicate glasses [11], ZnO-B_2O_3-PbO glasses [12], B_2O_3–Bi_2O_3–SrO glasses modified with Nd_2O_3 [13], PbO– B_2O_3–ZnO glass [14], ZnO–TeO_2–P_2O_5-ZnX glasses [15], GeO_2-B_2O_3-P_2O_5-ZnO-Tb_2O_3-RE magneto-optical glasses [16], molybdenum rich glass composite [17].

The high radiation absorption ability of lead (Pb) elements and various oxide components has highlighted the use of lead-containing protective clothing as shielding material, especially in medical applications [18],[19]. However, as lead is a toxic material, its use was restricted in many areas and even banned in some areas by the United States Congress in 1976 due to its harmful effects on human health and the environment [20]. New composite materials have been produced by reducing the Pb content in protective materials and mixing different materials. In this way, have been reduced the toxic effect of Pb. For example, with the mixture consisting of Ba, Sn, and I mixed with Pb, an absorption equivalent to lead have achieved and a lightness of 20–30% [21]. With epoxy resin [Mkhaiber and Dheyaa, [22] has compared using lead and lead-free composite materials [23]. In another study, the amount of radiation in mammography shots of PbO_2 samples of different thicknesses and the radiation absorption properties with the ISO s-^{137}Cs (662 keV) source have investigated [24].

Zirconium diboride (ZrB_2) is an ultra-high temperature ceramic with a melting temperature of 3245 °C and a low coefficient of thermal expansion. Furthermore, it is preferred in the aviation industry and space studies due to its high strength, rigidity, chemical stability, thermal shock resistance, low electrical resistance, high voltage capacity, thermal conductivity, anti-corrosion property, and neutron absorption capacity. Because of these properties, it is shown as a candidate for use in shielding applications and nuclear reactors [25, 26],Fahrenholtz and Hilmas, [27, 28].

For this reason, in this study, glass samples were coated with a solution prepared with 50%ZrB_2.50%PbO [27]. In addition, the second glass material was prepared by adding CuO, ZnO, and TiO_2 at a ratio of 1:1:3 to the obtained 50%ZrB_2.50%PbO mixture, respectively.

2 Materials and methods

2.1 Solution preparation and glass coating

Nanoparticle-sized oxide compounds need to be made into solution in order to be coated on the glass surface. The solution preparation process of oxide powders is described below [29, 30].

2.1.1 Preparation of PbO solution

Lead(II) oxide powder, < 10 µm, Reagent Plus®, ≥ 99.9% trace metals powder was used. To form a solution, PbO powders were mixed with ethanol, isopropanol alcohol, and PMMA liquid components for two days at room temperature to form a homogeneous mixture. Thin films were drip-coated onto glass substrates and allowed to dry.

2.1.2 Preparation of TiO_2 solution

Titanium Dioxide (TiO_2) Nano Powder, Purity: 99.995%, Size: 17 nm, and titanium n-butoxide was mixed with ethanol, isopropanol alcohol, and PMMA at the ratios of 1:20:20:0.15, respectively, to prepared TiO_2 solution. The mixture was stirred for two days at room temperature with a magnetic stirrer.

2.1.3 Preparation of ZnO solution

Zinc oxide Reagent Plus®, powder, < 5 µm particle size, 99.9% purity ZnO powder to prepare a solution, 2.5 ml of ethylene glycol, 1 ml of PMMA was added into 10 g of zinc acetate dihydrate in a round-bottomed flask and to obtain a homogeneous solution was stirred at room temperature for two days. The mixture, which changed from transparent to white after two days, was coated on glass substrates with the rotational coating method at 1800 rpm.

2.1.4 Preparation of CuO solution

Nano Powder, Purity: 99.5%, Size: < 77 µm particle size, CuO powders, ethanol, isopropanol alcohol, and PMMA were mixed for two days at room temperature to obtain a homogeneous mixture. It was coated on the glass by the rotational coating method with a rotational speed of 2500 r/min. It was left to dry for 24 h.

2.1.5 Preparation of ZrB_2 solution

Micron Powder, Purity: 99.5%, Size: 5.5 µm ZrB_2 nanoparticles were mixed with ethanol, isopropanol, and PMMA liquid components for two days at room temperature to form a homogeneous mixture. Thin films were coated at 1800 rpm by dripping onto glass substrates and left to dry for 24 h.

Taking 50% of the prepared ZrB_2 and PbO solutions (50%ZrB_2.50%PbO, Sample A), they were mixed for two days at room temperature and turned into a homogeneous mixture, and the glasses were coated with the rotational coating method. The resulting glasses were left to dry for one day. The resulting 50% solution was mixed with 1:1:3 ZnO, CuO, and TiO_2 solutions (50%$ZrB_2$50%PbO. 10%CuO.10%ZnO.30%TiO_2, Sample B) and mixed with magnetic fish for two days for homogeneous. The resulting homogeneous quintuple mixture was coated on the glass substrate at 1800 rpm by a rotational coating method and left to dry for 24 h. Mixing ratios and density values of the coated materials have described in Table 1.

Theoretical process (XCOM and GATE Simulation) was performed as described in previous studies (A. [27, 29–31]).

2.2 Radiation shielding parameters

The experimental setup as shown in Fig. 1 was established for measurement procedure and a collimator was designed to minimize the scattered beam based on the sample area. More details for the experimental setup were described in the previous study [30, 32].

The linear attenuation coefficient (LAC) of the glass samples was examined using Beer Lambert's law given in Eq. (1) and mass attenuation coefficient

Table 1 Mixing ratios and density values of the coated materials

Sample ID	PbO	ZnO	ZrB_2	TiO_2	CuO	50%ZrB_2.50%PbO	Intensity
Sample A	%50	0	%50	0	0	0	7.80 g/cm^3
Sample B	0	%10	0	%30	%10	%50	6.31 g/cm^3

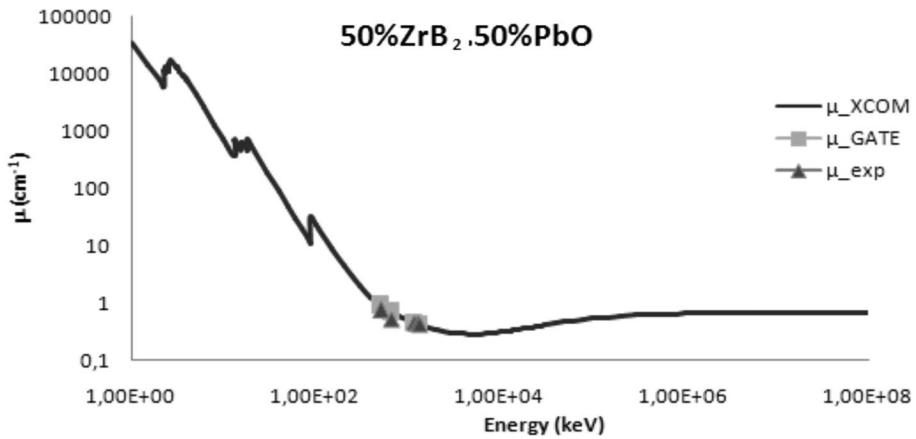

Fig. 1 Experimental and theoretical LAC values of Sample A mixture

(MAC) given in Eq. (2). Additionally, other relevant parameters such as HVL and MFP have been obtained using Eq. (3) and Eq. (4), respectively.

$$\mathrm{LAC} = \frac{1}{x}\,\mathrm{In}\,(\frac{I_0}{I}) \tag{1}$$

LAC is the linear attenuation coefficient in this equation, where x represents the thickness of the material, I represent the amount of gamma rays reaching the detector after interacting with it, and I_0 is the number of gamma rays reaching the detector without interacting with the material [33].

The mass attenuation coefficient (MAC) determines the ease with which a radiation beam can penetrate a material and it has given by Eq. (2). ϱ is the density of the material [9],

$$MAC = LAC/\rho \tag{2}$$

The Half Value Layer (HVL), which is used to halve the incident gamma radiation, can be determined using the Eq. (3) [10],

$$HVL = ln(2)/LAC \tag{3}$$

Mean Free Path (MFP) is the average distance the gamma ray moves without interacting with the material, and it is given in Eq. (4) [8],

$$MFP = 1/LAC \tag{4}$$

3 Results and discussion

The linear attenuation coefficients (LAC) for Sample A (50%ZrB_2.50%PbO) and the Sample B (50%$ZrB_2$50%PbO.10%CuO.10%ZnO. 30%TiO_2) were measured at 511, 662, 1173, 1275 and 1332 keV gamma energies emitted from ^{22}Na, ^{137}Cs and ^{60}Co radioactive sources.

Table 2, Fig. 1 and Fig. 2 showed that the experimental and theoretical LAC values of samples, respectively. Also, experimental LAC values for Sample A and Sample B have been shown that Fig. 3. It can be clearly seen from Table 2 and Fig. 3 that the linear attenuation coefficients decreased with the increasing gamma ray energies.

The LAC for samples at 5 different gamma energies was measured to obtain the Mean Free Path (MFP).

Table 2 Experimental and theoretical LAC values of sample A and sample B for all energies

	LAC_{-exp} (cm^{-1})		LAC_{-GATE} (cm^{-1})		LAC_{-XCOM} (cm^{-1})	
Energy	Sample A	Sample B	Sample A	Sample B	Sample A	Sample B
511 keV	0.749	0.623	0.921	0.700	0.920	0.675
632 keV	0.522	0.552	0.708	0.552	0.704	0.541
1173 keV	0.463	0.377	0.452	0.350	0.449	0.365
1274 keV	0.446	0.363	0.428	0.352	0.425	0.347
1332 keV	0.417	0.320	0.417	0.337	0.414	0.338

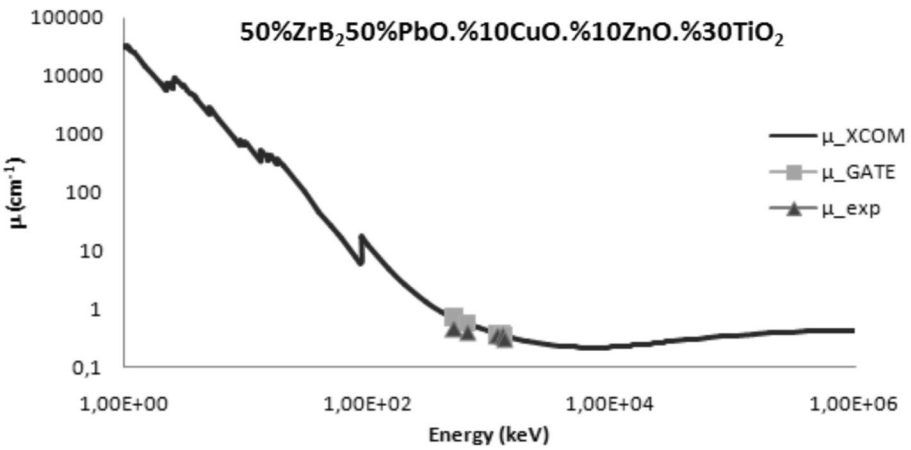

Fig. 2 Experimental and theoretical LAC values of Sample B mixture

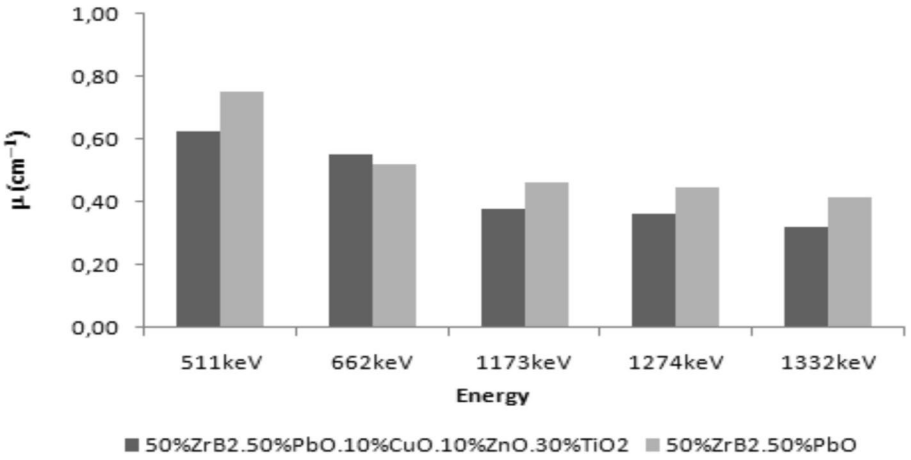

Fig. 3 Experimental LAC values for Sample A and Sample B

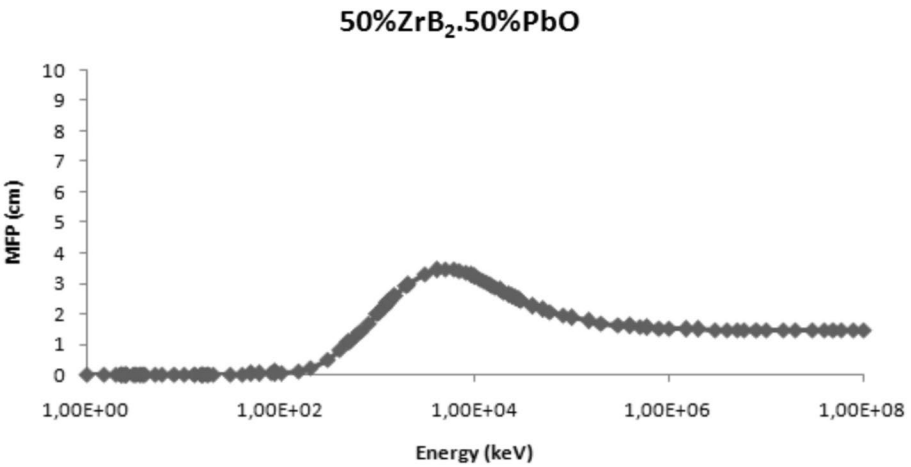

Fig. 4 Theoretical MFP values of Sample A mixture

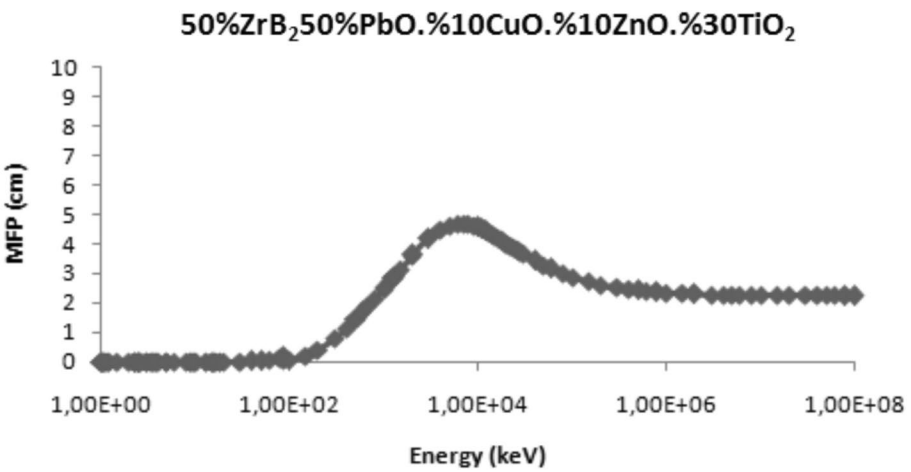

Fig. 5 Theoretical MFP values of Sample B mixture

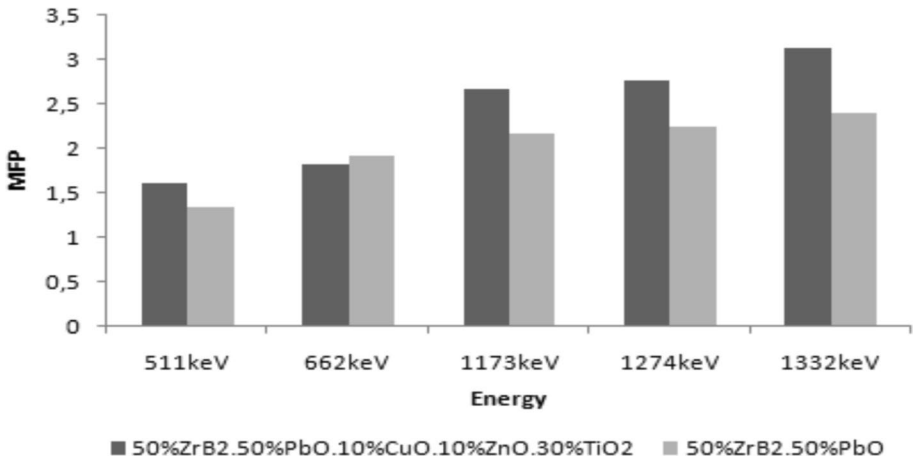

Fig. 6 Experimental MFP values for Sample A and Sample B

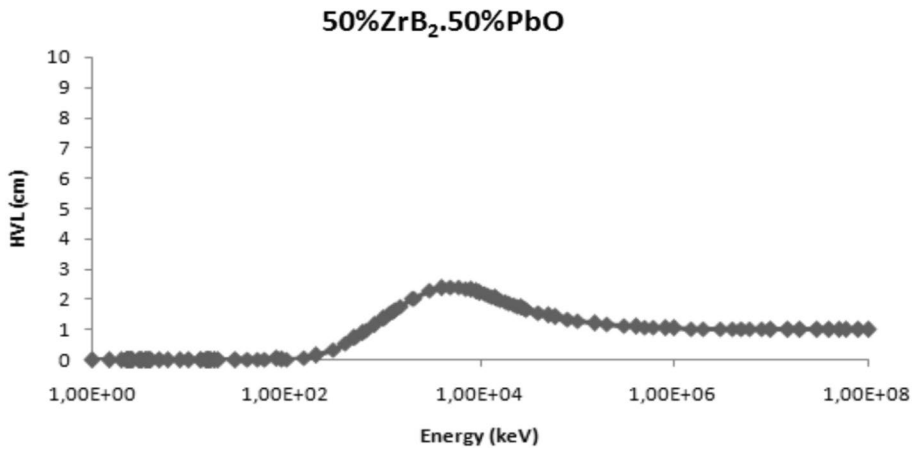

Fig. 7 Theoretical HVL values of Sample A mixture

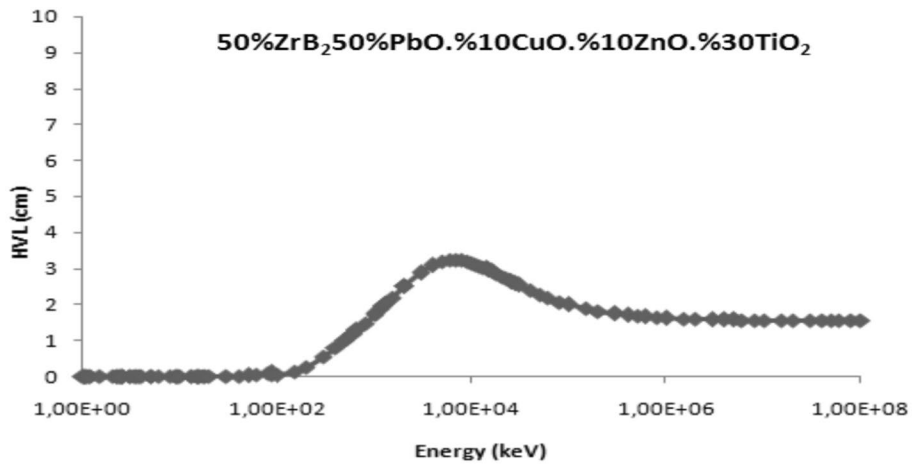

Fig. 8 Theoretical HVL values of Sample B

Figure 4 and Fig. 5 have been showed that the theoretical MFP values of the materials. Also, experimental MFP values for Sample A and Sample B have been shown that Fig. 6. It can be clearly seen from Fig. 6, during the low energy gamma is able to lose their energy at a short distances, while the high energy gamma is able to lose their energy at a longer distance.

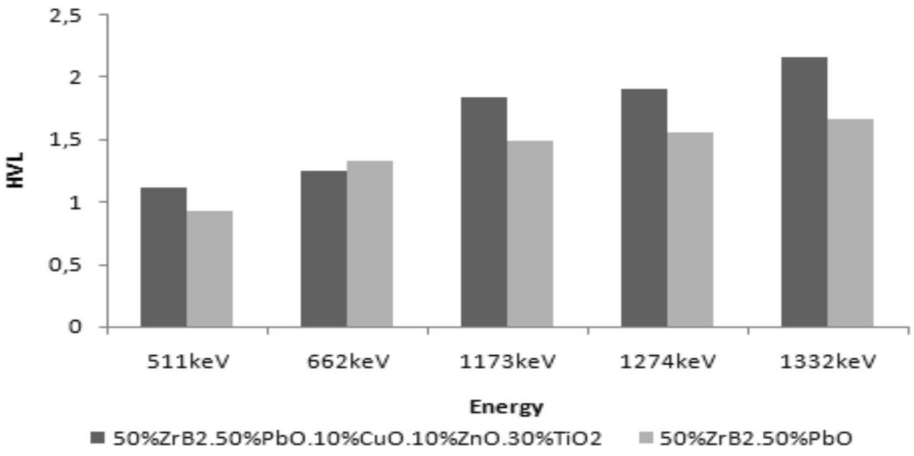

Fig. 9 Experimental HVL values of Sample A and Sample B

Figure 7 and Fig. 8 have been showed that the theoretical Half Value Layer (HVL) values of the materials. Also, it was shown that in Fig. 9, the thicknesses needed to decrease the incoming gamma radiation intensity of experimental HVL values for Sample A and Sample B. According to Fig. 9, it is seen that HVL rises with the increase in gamma energy.

4 Conclusion

This study, which was conducted to contribute to the literature and develop new radiation absorbing materials, included experimental measurements as well as theoretical calculations such as the GATE simulation program and the XCOM program. LAC, HVL, and MFP of the Sample A (50%ZrB_2.50%PbO) and the Sample B (50%$ZrB_2$50%PbO.10%CuO.10%ZnO.30%TiO_2) have been calculated. The LAC of the Sample A and Sample B were determined using three gamma point sources such as ^{22}Na (511 and 1274 keV), ^{137}Cs (662 keV) and ^{60}Co (1173 and 1332 keV).

As a result of the study, the linear absorption coefficient of uptake appears to diminish as the energy increases. Also, the experimental data have been found to be compatible with the Gate and XCOM simulation programs. While the linear absorption coefficient is high at low energy levels, the HVL and MFP values decrease. The linear absorption coefficient decreases at high energy values due to the dominance of Compton scattering. Especially when looking at Fig. 3, it is seen that with the addition of the mixture in a ratio of 1:1:3 (Sample B), it exhibits lower absorption properties than the Sample A. While the LAC values of the Sample A were 0.75 cm^{-1} at 511 keV energy, it decreased to 0.62 cm^{-1} in the Sample B. At 1332 keV energy value, it decreases from 0.42 cm^{-1} to 0.32 cm^{-1} in Sample A and Sample B, respectively. While the HVL and MFP values are high in the Sample B, the values of the Sample A decrease.

Authorship contribution

[A. Poyraz]: Data curation, Formal analysis, Methodology, Software, Writing original draft. [I. Yigitoglu]: Data curation, Formal analysis, Methodology. [B. Canimkurbey]: Resources, Validation, Investigation. [B. Cetin]: Conceptualization, Data curation, Validation, Investigation, Methodology, Resources, Supervision, Visualization, Writing original draft, Writing—review & editing.

Funding

Open access funding provided by the Scientific and Technological Research Council of Türkiye (TÜBİTAK). This study received no specific funding from the public, commercial or not-for-profit sectors.

Data availability

The datasets generated and analyzed during the current study are available from the corresponding author upon reasonable request. This manuscript complies with the Springer Nature Research Data Policy. All relevant data related to the findings are included in the

manuscript and additional data can be shared upon request, ensuring transparency and reproducibility.

Declarations

Conflict of interest The authors declare that they have no known competing financial interests or personal relationships that could have appeared to influence the work reported in this paper.

Open Access This article is licensed under a Creative Commons Attribution 4.0 International License, which permits use, sharing, adaptation, distribution and reproduction in any medium or format, as long as you give appropriate credit to the original author(s) and the source, provide a link to the Creative Commons licence, and indicate if changes were made. The images or other third party material in this article are included in the article's Creative Commons licence, unless indicated otherwise in a credit line to the material. If material is not included in the article's Creative Commons licence and your intended use is not permitted by statutory regulation or exceeds the permitted use, you will need to obtain permission directly from the copyright holder. To view a copy of this licence, visit http://creativecommons.org/licenses/by/4.0/.

References

1. I. Akkurt, H. Akyıldırım, B. Mavi, S. Kilincarslan, C. Basyigit, Radiation shielding of concrete containing zeolite. Radiat. Meas.. Meas. **45**(7), 827–830 (2010). https://doi.org/10.1016/j.radmeas.2010.04.012
2. B. Mavi, Experimental investigation of γ-ray attenuation coefficients for granites. Ann. Nucl. EnergyNucl. Energy **44**, 22–25 (2012). https://doi.org/10.1016/j.anucene.2012.01.009
3. M. Ni, X. Tang, H. Chai, Y. Zhang, T. Chen, D. Chen, Preparation and properties of the fast-curing γ-ray-shielding materials based on polyurethane. Nucl. Eng. Technol.. Eng. Technol. **48**(6), 1396–1403 (2016). https://doi.org/10.1016/j.net.2016.06.008
4. H. Binici, O. Aksogan, A.H. Sevinc, A. Kucukonder, Mechanical and radioactivity shielding performances of mortars made with colemanite, barite, ground basaltic pumice and ground blast furnace slag. Constr. Build. Mater. **50**, 177–183 (2014). https://doi.org/10.1016/j.conbuildmat.2013.09.033
5. B. Cetin, Ş Yalçin, B. Aktas, M. Albaşkara, Investigation of radiation shielding properties of soda-lime-silica glasses doped with different food materials. Acta Phys. Pol., A **132**(3), 988–990 (2017). https://doi.org/10.12693/APhysPolA.132.988
6. A.M. Babeer, M.I. Sayyed, H.Y. Morshidy, A.E.R. Mahmoud, M.A. Abdo, M.S. Sadeq, High transparency of PbO–BaO–Fe2O3–SrO–B2O3 glasses with improved radiation shielding properties. Opt. Mater.Mater. **145**, 114387 (2023). https://doi.org/10.1016/j.optmat.2023.114387
7. A. Coşkun, B. Cetin, The effect of lead oxide on the change in gamma ray protection parameters of bismuth oxide. Avrupa Bilim ve Teknoloji Dergisi **47**, 18–21 (2023)
8. V.P. Singh, N.M. Badiger, J. Kaewkhao, Radiation shielding competence of silicate and borate heavy metal oxide glasses: comparative study. J. Non-Cryst. SolidsCryst. Solids **404**, 167–173 (2014). https://doi.org/10.1016/J.JNONCRYSOL.2014.08.003
9. S. Kaewjang, U. Maghanemi, S. Kothan, H.J. Kim, P. Limkitjaroenporn, J. Kaewkhao, New gadolinium based glasses for gamma-rays shielding materials. Nucl. Eng. Des.. Eng. Des. **280**, 21–26 (2014). https://doi.org/10.1016/j.nucengdes.2014.08.030
10. M.I. Sayyed, Bismuth modified shielding properties of zinc boro-tellurite glasses. J. Alloy. Compd. **688**, 111–117 (2016). https://doi.org/10.1016/j.jallcom.2016.07.153
11. Y.S. Rammah, A. Kumar, K.A.A. Mahmoud, R. El-Mallawany, F.I. El-Agawany, G. Susoy, H.O. Tekin, SnO-reinforced silicate glasses and utilization in gamma-radiation-shielding applications. Emerg. Mater. Res. **9**(3), 1000–1008 (2020). https://doi.org/10.1680/jemmr.20.00150
12. M.I. Sayyed, Y.S. Rammah, A.S. Abouhaswa, H.O. Tekin, B.O. Elbashir, ZnO-B2O3-PbO glasses: synthesis and radiation shielding characterization. Physica B B **548**, 20–26 (2018). https://doi.org/10.1016/j.physb.2018.08.024
13. H.H. Hegazy, M.S. Al-Buriahi, F. Alresheedi, F.I. El-Agawany, C. Sriwunkum, R. Neffati, Y.S. Rammah, Nuclear shielding properties of B2O3–Bi2O3–SrO glasses modified with Nd2O3: theoretical and simulation studies. Ceram. Int.Int **47**(2), 2772–2780 (2021). https://doi.org/10.1016/j.ceramint.2020.09.131
14. J. Shi, L. Wang, H. Xie, S. Yao, X. Pu, Z. Liu, Y. Ding, Effect of PbO on the chemical durability of low-temperature PbO–B2O3–ZnO glass for cesium immobilization. Ceram. Int. (2024). https://doi.org/10.1016/j.ceramint.2024.02.349
15 G. Kilic, E. Ilik, E. Kavaz, G. Almisned, D.S. Baykal, H.O. Tekin, Mechanical, gamma rays and neutron radiation

transmission properties for some ZnO–TeO2–P2O5-ZnX glasses. Ceram. Int. **49**(19), 31773–31783 (2023). https://doi.org/10.1016/j.ceramint.2023.07.132

16. G. ALMisned, D.S. Baykal, E.R.K.A.N. Ilik, M. Abuzaid, G. Kilic, H.O. Tekin, Functional assessment of various rare-earth (RE) ion types: an investigation on gamma-ray attenuation properties of GeO2-B2O3-P2O5-ZnO-Tb2O3-RE magneto-optical glasses. Optik **274**, 170526 (2023)
17. T. Zagyva, F.E. Kaufmann, S. de MoraesShubeita, L. Leay, M. Harrison, T. Taylor, B. O'Driscoll, Microstructure and radiation tolerance of molybdenum-rich glass composite nuclear waste forms. J. Nucl. Mater.Nucl. Mater. **585**, 154635 (2023)
18. H. Eder, W. Panzer, H. Schöfer, Is the lead-equivalent suited for rating protection properties of lead-free radiation protective clothing. RoFo: Fortschritte Auf Dem Gebiete Der Rontgenstrahlen Und Der Nuklearmedizin **177**(3), 399–404 (2005). https://doi.org/10.1055/s-2005-857885
19. Ballsieper, B. 2008. Radiation protection material based on silicone. U.S. Patent No. 7,432,519. 7 Oct. 2008.
20. D.N. Dodoo-Amoo, S. Landsberger, J.M. MacDonald, J.M. Castro, Development of composite materials for non-leaded gloves for use in radiological hand protection. Health Phys. **84**(6), 737–746 (2003). https://doi.org/10.1097/00004032-200306000-00006
21. ICRP, 2007. The 2007 Recommendations of the International commission on radiological protection. ICRP publication 103. Ann. ICRP 37 (2–4).
22. A.F. Mkhaiber, A. Dheyaa, Experimental study of some shielding parameters for composite shields. J. Phys. Conference Ser. **1003**(1), 012109 (2018)
23. H. Eder, H. Schlattl, C. Hoeschen, X-Ray protective clothing: does DIN 6857–1 allow an objective comparison between lead-free and lead composite materials? RoFo - Fortschritte Auf Dem Gebiet Der Röntgenstrahlen Und Der Bildgebenden Verfahren **182**(05), 422–428 (2010). https://doi.org/10.1055/s-0028-1110000
24. Demirel, I. 2019. Development of novel shielding material based on epoxy matrix loaded by high-Z chemical powders used for mammographic, diagnostic and industrial X and gamma ray energy range, and determination of its photon attenuation properties by ionization chamber method with use of standard beam qualities. Ankara University Master Thesis, 68s.
25. O. Balcı, N. Akçamlı, D. Ağaoğulları, M.L. Öveçoğlu, I. Duman, Autoclave processing and sintering of ZrB_2-ZrO_2 powders and investigation of microstructural and some mechanical properties of bulk products. J. of Boron **2**(1), 1–10 (2017)
26. A.L. Chamberlain, W.G. Fahrenholtz, G.E. Hilmas, D.T. Ellerby, High-strength zirconium diboride-based ceramics. J. Am. Ceram. Soc. **87**(6), 1170–1172 (2004). https://doi.org/10.1111/j.1551-2916.2004.01170.x
27. A. Coşkun, B. Çetin, I. Yiğitoğlu, H. Topaklı, Comparison of the radiation absorption properties of PbO doped ZrB_2 glasses by using GATE-GEANT4 monte carlo code and XCOM program. Int. J. of Computational and Experimental Sci. Eng. **9**(3), 274–279 (2023). https://doi.org/10.22399/ijcesen.1338491
28. W.G. Fahrenholtz, G.E. Hilmas, Oxidation of ultra-high temperature transition metal diboride ceramics. Int. Mater. Rev. **57**(1), 61–72 (2012). https://doi.org/10.1179/174328041Y.0000000012
29. Coşkun, A. 2023. Experimental and theoretical calculation of the radiation shielding values of some metal containing composites. Amasya University Doctoral Thesis, 122s.
30. A. Coşkun, B. Çetin, I. Yiğitoğlu, B. Canımkurbey, Theoretical and experimental investigation of gamma shielding properties of TiO_2 and PbO coated glasses. Int. J. Computational and Experimental Sci. Eng. **9**(4), 398–401 (2023). https://doi.org/10.22399/ijcesen.1367747
31. A. Coşkun, I. Yiğitoğlu, H. Topakli, B. Cetin, Determination of the radiation shielding performance of MoO_2 addition on PbO by monte carlo simulation. Int. Conference on Pioneer and Innovative Stud. **1**, 223–227 (2023). https://doi.org/10.59287/icpis.834
32. Y. Savaş, B. Başaran, B. Çetin, The effect of marble powder additive at different ratios on the radiation absorption parameters of barite based concretes. Int. J. Computational Experimental Sci. Eng. **9**(4), 376–381 (2023). https://doi.org/10.22399/ijcesen.1322248
33. K.S. Krane, W.G. Lynch, Introductory nuclear physics. Phys. Today (1989). https://doi.org/10.1063/12810884

Publisher's Note Springer Nature remains neutral with regard to jurisdictional claims in published maps and institutional affiliations.